

Collider Phenomenology of $e^-e^- \rightarrow W^-W^-$

Kai Wang, Tao Xu, and Liangliang Zhang

Zhejiang Institute of Modern Physics and Department of Physics,

Zhejiang University, Hangzhou, Zhejiang 310027, China

Abstract

Whether in nature exists Majorana neutrino is one of the most fundamental questions in physics. It is directly related to the violation of accidental $U(1)$ -lepton number symmetry(LNV). Enormous efforts had been put into such test and among them, one conventional experiment is the neutrinoless double-beta decay ($0\nu\beta\beta$). On the other hand, there have been proposals of future electron-positron colliders such as International Linear Collider (ILC) for precision measurements of Higgs boson or new discovered beyond SM particles and it can potentially be converted into an electron-electron collider. Such collider enables a new probe of Majorana neutrino via the inverse $0\nu\beta\beta$ process($e^-e^- \rightarrow W^-W^-$) as an alternative and complementary test to the conventional neutrinoless double-beta decay experiments. In this paper, we illustrate the searching strategies of $e^-e^- \rightarrow W^-W^-$ at future electron colliders, and find that the channels of pure hadronic, semi-leptonic with muon and pure leptonic with muons have the most discovery potential.

I. INTRODUCTION

Enormous neutrino oscillation experiments in the last two decades have provided definite evidence for non-zero neutrino masses and the mixing between different flavors [1–3]. This becomes the first hint that the Standard Model (SM) of particle physics must be extended. Meanwhile, the Higgs boson is the last building block of SM and its discovery has significantly improved our knowledge over spontaneous electroweak symmetry breaking. However, the origin of neutrino mass as one of the motivations to go beyond it, remains an open question. The neutrino could have a Dirac mass through Yukawa mechanism like other SM fermions. But, first of all, the hierarchy in y_ν/y_t at $\mathcal{O}(10^{-12})$ is quite unnatural. A second argument arises from the prediction of electric charge quantization. The bound on neutrino electric charge Q_ν is $|Q_\nu| \lesssim (0.5 \pm 2.9) \times 10^{-21}e$ (68% CL, e is the magnitude of the electronic charge) by assuming charge conservation in β -decay $n \rightarrow p + e^- + \bar{\nu}_e$ [4, 5], and $|Q_\nu| < 2 \times 10^{-15}e$ from SN1987A astrophysics observation [6]. Anomaly-free conditions determine $U(1)_Y$ as the unique $U(1)$ gauge symmetry in SM up to a normalization factor [7]. Though extending SM with milli-charged Dirac neutrino does not explicitly violate the anomaly-free conditions, the hyper-charge assignment is no longer unique unless the neutrino is a Majorana particle [8]. These motivate the study of Majorana neutrinos.

Taking the effective theory approach, Majorana neutrino mass term is from the non-renormalizable Weinberg operator $(y_{ij}/\Lambda_\ell)\ell_i\ell_j\Phi\Phi$ [9] where y_{ij} is dimensionless. This dimension-five operator breaks $U(1)_L$ Lepton Number by two units ($\Delta L = 2$), indicating new physics comes in at Λ_ℓ scale. Being remanent of the global chiral symmetry, Lepton Number and Baryon Number arise as accidental symmetries which would be violated by non-perturbative gravitational effects at the Planck's scale M_{Pl} . However, if one identify M_{Pl} as the Λ_ℓ scale, the neutrino mass is only of order 10^{-5} eV, which is much too small to explain for the observed oscillation phenomenon. Another possibility is that $\mathcal{O}(\text{eV})$ neutrino mass is a consequence of M_{GUT} suppression since the grand unification theory (GUT) scale is several orders lower than M_{Pl} . The simplest realization is the so-called type-I “see-saw” mechanism where a SM singlet neutrino N forms Dirac mass term with lepton $SU(2)_L$ doublet as $y_\nu \bar{\ell}_L N \Phi$ and a Majorana mass term by itself $M_R \bar{N}^c N$ [10–13]. The lighter mass eigenstates are then identified as the light neutrinos and the heavy ones with mass M_N are still in search. The SM singlet N can be accommodated in the spinor representation of $SO(10)$ GUT group as $16 = 10 + \bar{5} + 1$. In such GUT-models, M_R spontaneously breaks the $U(1)_{B-L}$ gauge symmetry. Further possibility exists in extended models where

a higher-dimensional Weinberg operator $[\mu_{ij}^{(n-1)}/\Lambda^n]\ell_i\ell_j\Phi\Phi$ allows more freedom in choosing Λ scale and μ coefficient for correct neutrino mass.

Neutrionless double beta decay ($0\nu\beta\beta$) is the most important experiment to test such $\Delta L = 2$ process. So far there's no $0\nu\beta\beta$ signal observed by GERDA and KamLAND-Zen collaborations, which put lower half-life limits on ^{76}Ge and ^{136}Xe isotopes [14, 15]. These results provide the strongest bound on the mixing V_{eN} between electron and heavy Majorana neutrinos as $|V_{eN}|^2 \leq 10^{-8}$ - 10^{-6} for a wide M_N window ranging from 1 MeV to 500 GeV. However, the existence of Majorana CP phases could cause cancellation between amplitudes in $0\nu\beta\beta$ process and this significantly weaken the exclusion limits when there're more than two sterile Majorana neutrino flavors [16, 17]. There are also direct or indirect searching experiments that put constraints on the mixings at different M_N regions from eV to TeV[19–36]. Related phenomenological analysis could be found in [37–39]. The direct production of heavy neutrino on colliders makes the searches possible in both precision frontier and energy frontier. Experiments with abundant mesons could probe mass region smaller than meson masses in process $X^\pm \rightarrow \ell^\pm \nu_N$. The decay branching ratio is proportional to the mixing $|V_{\ell N}|^2$ and the lepton energy spectrum deviates from the usual case with light active neutrinos. If the heavy neutrinos are Majorana particles, their LNV decays into same-sign leptons could further be detected. In LHCb and BELLE experiments where precise measurement of B -meson decay is available, constrains on the mixing $|V_{\ell N}|^2$ from LNV decay search is around $\mathcal{O}(10^{-4})$ when M_N is close to m_B [19, 20]. In the case when M_N is smaller than m_D , the so-called beam dump search experiments could detect the decay final states of those ν_N coming from D -mesons. The CHARM and NuTeV experiments each could push the upper limit of $|V_{eN}|^2$ and $|V_{\mu N}|^2$ down to below 10^{-6} while the PS191 and E949 bounds in the region below 450 MeV are even stronger[21–25]. The most severe bound in this region is close to 10^{-9} when M_N is around 300 MeV. The E_ℓ peak search, for example in the $\pi \rightarrow e\nu_N$ [31] and $K \rightarrow \mu\nu_N$ [32] processes, could be used in the very small mass region below that. Collider experiments at the energy frontier could also probe the heavy Majorana particles. The DELPHI experiment at LEP put upper limit to $Z \rightarrow \nu_N\nu$ decay branching ratio for M_N between 3.5 and 50 GeV through the measurement of Z decay and $|V_{\ell N}|^2$ upper bound is set at $\mathcal{O}(10^{-5})$ [33]. Further large mass regions are in the reach of the hadron colliders. The smoking gun signature is same-sign dilepton plus jets with no \cancel{E}_T . Both the ATLAS[34] and the CMS[35, 36] collaborations have published the result with 8 TeV data for M_N up to 500 GeV. However, this is still weaker than the electroweak precision observables (EWPO) bound, which is sensitive to the non-unitarity of leptonic mixing

matrix [40]

$$\sum_i |V_{ei}|^2 \leq |V_e|_{EW}^2 = 2.1 \times 10^{-3}. \quad (1)$$

Recently, several future electron-positron colliders have been proposed for precise Higgs measurement. Such machine may enable the inverse $0\nu\beta\beta$ process as $e^-e^- \rightarrow W^-W^-$ (Fig.1) to probe Majorana neutrino. This could become an alternative and complementary experiment to the conventional $0\nu\beta\beta$ because the energy scales are different. Previous studies in related topics could be found in [41–52]. In this paper, we focus on the collider phenomenology and searching strategies of $e^-e^- \rightarrow W^-W^-$.

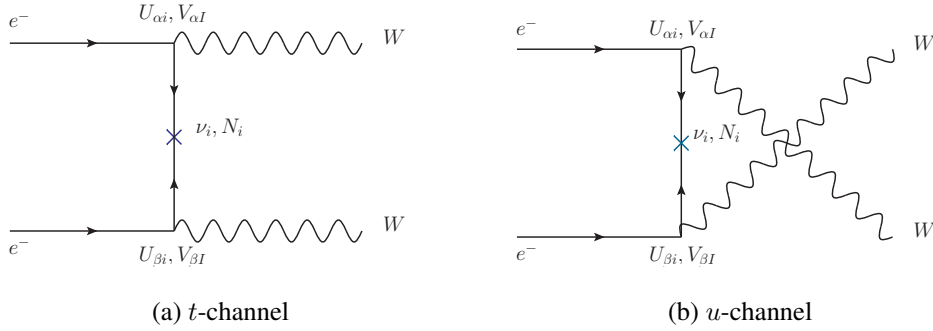


FIG. 1: inverse $0\nu\beta\beta$ decay

II. SIGNAL AND BACKGROUND

The $e^-e^- \rightarrow W^-W^-$ scattering could be measured in three decay modes as pure leptonic, semi-leptonic and pure hadronic. In the following, we will first discuss the kinematic features of each modes for experimental measurements.

In the pure leptonic mode, the two final state leptons always move back-to-back with each other as W^-W^- is from a spin-zero system and only left-handed electrons take part in the weak interaction. This leads to an angular-distribution which peaks at $\cos \theta_{ll} = -1$. The $\cos \theta_{ll}$ cut could be applied to distinguish signals from backgrounds.

On the other hand, the two invisible neutrino final states make it impossible to reconstruct the two W bosons with E_T information. M_{T2} method could be used here by defining a minimization of all possible matches of \not{p}_1 and \not{p}_2 variables as [53]

$$M_{T2}^2 \equiv \min_{\not{p}_1 + \not{p}_2 = \not{p}_T} \left[\max \{ m_T^2(p_T^\ell, \not{p}_1), m_T^2(p_T^\ell, \not{p}_2) \} \right] \quad (2)$$

where \cancel{p}_T is the missing transverse momentum and m_T is the reconstructed transverse mass. The M_{T2} variable has an upper bound at m_W and the corresponding $\cancel{p}_{1,2}$ could be used in reconstructing the system invariant-mass, whose distribution is around \sqrt{s} in signal events. Moreover, if the electron collider could be upgraded to a few-TeV machine, the distinct boosted properties of final states allow us more kinematic handles on data sample reconstruction. We thus treat the highly boosted leptons and neutrinos from a same W boson as they're approximately collinear. Then the approximate relation $\vec{p}_\nu = \kappa \vec{p}^\ell$ could be used to solve for the two neutrinos as

$$\kappa = \frac{\cancel{p}_T}{p_T^{\ell_1} + p_T^{\ell_2}} \quad (3)$$

If all the final states are obtained in this approximation, the invariant-mass cut could still be applied.

The semi-leptonic decay has larger signal production cross-section than the pure leptonic mode and it's more reconstructable. Since the two beams are symmetric, the momentum of the only neutrino is just

$$\vec{p}_\nu = - \sum_i \vec{p}_{observed}$$

The two on-shell W bosons could be reconstructed either with a proper pair of jets or with the lepton and neutrino.

In the hadronic mode with multi-jet final states, the W bosons could be reconstructed with proper choices of jet-pairs and the invariant-mass of the two pairs of jets is to be compared with \sqrt{s} for event selection. If the collision is energetic enough, the boost effect could be prominent as two jets from a boosted W would form a fat W -jet(j_W) with jet mass around 80 GeV. The appearance of two W -jets is a key feature of hadronic decay at high collision energy.

The backgrounds of this process and the decay channels they contribute to are listed in Table.I below. We include processes with extra electrons because of the abundance of background electrons on this ee -collider. These extra electrons could fake \cancel{E}_T if they are not really detected, especially in the effective gauge-boson approximation and vector boson fusion process. The radiated photons from leptons are also taken into consideration because the cross-section could be comparable with other channels. Its contribution is calculated in the Effective Photon Approximation with the improved Weizsaecker-Williams formula[54].

Process	$e^-e^- + \cancel{E}_T$	$e^-\mu^- + \cancel{E}_T$	$\mu^-\mu^- + \cancel{E}_T$	$e^- + 2j + \cancel{E}_T$	$\mu^- + 2j + \cancel{E}_T$	$4j$
$e^-e^- \rightarrow W^-W^-\nu_e\nu_e$	•	•	•	•	•	•
$e^-e^- \rightarrow ZW^-e^-\nu_e$	•	•		•	•	•
$e^-e^- \rightarrow W^-e^-\nu_e$	•	•		•		
$e^-e^- \rightarrow Ze^-e^-$	•			•		
$e^-e^- \rightarrow ZZe^-e^-$	•			•		•
$e^-e^- \rightarrow W^+W^-e^-e^-$				•	•	•
$\gamma\gamma \rightarrow W^+W^-$				•	•	•

TABLE I: Backgrounds of inverse $0\nu\beta\beta$ process and the decay channels

III. RESULT

In this section, we discuss the Monte Carlo analysis of inverse $0\nu\beta\beta$ process. The simulation is performed with *MadGraph5_v1.5.14*[55] and *pythia-pgs*[56]. We choose two benchmark points with $\sqrt{s} = 500$ GeV and $\sqrt{s} = 3$ TeV separately, in order to get more kinematic features from boost effects. According to the previous study[52], inverse $0\nu\beta\beta$ scattering signal with only one or two Majorana neutrino flavors are too small to be detected. For this reason, we include three heavy Majorana neutrinos in the spectrum as $M_1 = 3$ GeV, $M_2 = 350$ GeV and $M_3 = 35$ TeV when $\sqrt{s} = 500$ GeV while $M_1 = 3$ GeV, $M_2 = 3$ TeV and $M_3 = 300$ TeV when $\sqrt{s} = 3$ TeV. The hierarchical mass relation $M_1 \ll M_2 \ll M_3$ suppresses $|V_{e1}|^2$ and $|V_{e3}|^2$ to several orders smaller than $|V_{e2}|^2$, which we take the $|V_e|_{EW}^2$ value in (1) accordingly. The basic cuts on final states transverse momentum, rapidity and separations are

$$\begin{aligned}
p_T^\ell &> 10 \text{ GeV} , \quad p_T^j > 20 \text{ GeV}, \\
|\eta^\ell| &< 2.5 , \quad |\eta^j| < 5, \\
\Delta R_{\ell\ell} &> 0.4 , \quad \Delta R_{\ell j} > 0.4
\end{aligned} \tag{4}$$

In addition, the two selected jets in the first benchmark are required to satisfy $\Delta R_{jj} > 0.4$.

Fig.2 shows the dependence of SM backgrounds on \sqrt{s} . The cross-sections except for $e^-e^- \rightarrow ZZe^-e^-$ are always larger than 1 fb. In order to find out feasible discovery channels, we start event selection with the tagging process which requires proper final states in each channels. For example,

if more than required electrons are detected in the rapidity coverage region of the detector, they're supposed to come from background processes with extra electrons and thus we discard this event. After that, kinematic cuts are used to eliminate background events for better signal-to-background rate.

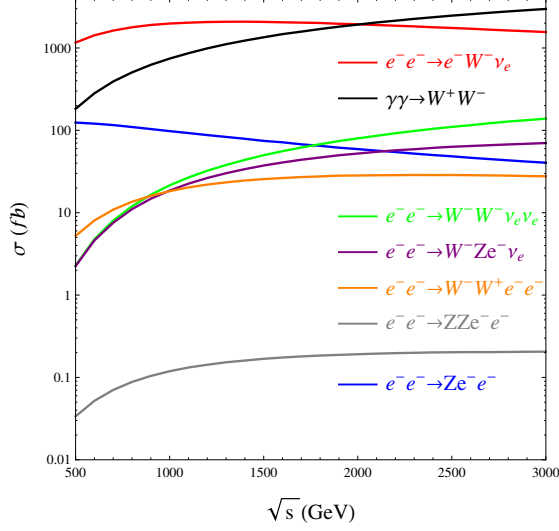
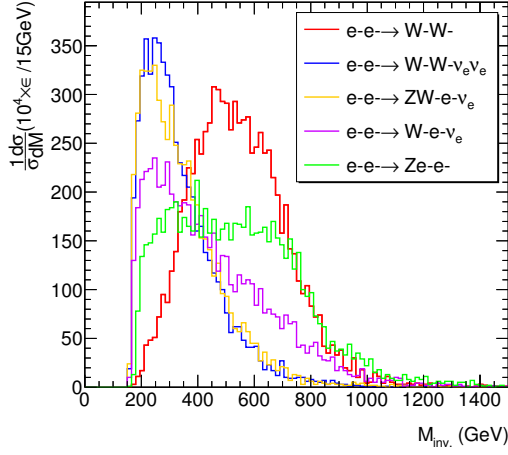


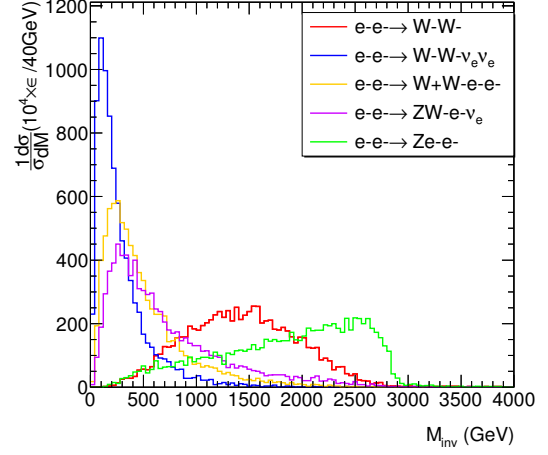
FIG. 2: SM background cross-sections with different \sqrt{s} values

A. Pure-leptonic mode

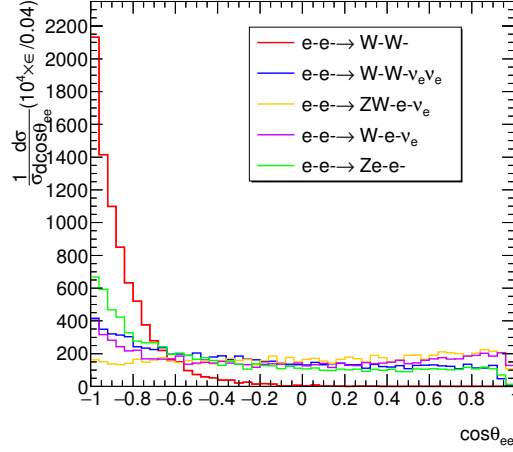
With M_{T2} method in the first benchmark and collinear approximation in the second, we plot the reconstructed invariant-mass m_{inv} distributions in the $e^-e^- + \cancel{E}_T$ channel, which includes most backgrounds, in Fig.3a and Fig.3b. In order to illustrate the lepton angular correlation feature, we plot the distribution in Fig.3c. It's shown in the figures that signal m_{inv} is larger than those of the backgrounds except for the Ze^-e^- process. Moreover, the leptons from Ze^-e^- tend more to move in the opposite directions compared with other backgrounds. However, this process should be absent in the $e^-\mu^-$ and $\mu^-\mu^-$ channels.



(a) m_{inv} distribution, $\sqrt{s} = 500$ GeV



(b) m_{inv} distribution, $\sqrt{s} = 3$ TeV



(c) $\cos \theta_{ee}$ distribution, $\sqrt{s} = 500$ GeV

FIG. 3: Kinematic features of signal and backgrounds in pure leptonic mode. ϵ is the tagging efficiencies

In Table.II and III, we list the cross-sections after basic cuts in (4) and the survival probabilities after kinematic cuts. The m_{inv} cut is different in electron and muon channels because of the contribution from different background processes. The $\cos \theta_{\ell\ell}$ cut in the second benchmark is more severe because the signal leptons are from more boosted W bosons. We assume the invariant-mass cut and $\cos \theta_{\ell\ell}$ cut are independent and results in the last column are the efficiencies under all cuts. The “—” means it’s not applicable in the corresponding case.

Process	σ	$\epsilon_{\text{tagging}}$	$\epsilon_{m_{\text{inv}} > 400 \text{ GeV}}$	$\epsilon_{\cos \theta_{ll} < -0.7}$
$e^-e^- + \cancel{E}_T$ channel				
$e^-e^- \rightarrow W^-W^-$	$5.0 \times 10^{-3} \text{ fb}$	0.84	0.68	0.591
$e^-e^- \rightarrow W^-W^- \nu_e \nu_e$	$2.57 \times 10^{-2} \text{ fb}$	0.83	0.15	0.042
$e^-e^- \rightarrow ZW^-e^- \nu_e$	$4.7 \times 10^{-2} \text{ fb}$	0.84	0.17	0.024
$e^-e^- \rightarrow W^-e^- \nu_e$	120.8 fb	0.83	0.3	0.069
$e^-e^- \rightarrow Ze^-e^-$	24.7 fb	0.84	0.5	0.185
$e^- \mu^- + \cancel{E}_T$ channel				
$e^-e^- \rightarrow W^-W^-$	$1.0 \times 10^{-2} \text{ fb}$	0.87	0.70	0.603
$e^-e^- \rightarrow W^-W^- \nu_e \nu_e$	$5.14 \times 10^{-2} \text{ fb}$	0.85	0.16	0.045
$e^-e^- \rightarrow ZW^-e^- \nu_e$	$4.7 \times 10^{-2} \text{ fb}$	0.85	0.17	0.024
$e^-e^- \rightarrow W^-e^- \nu_e$	120.8 fb	0.80	0.29	0.069
$\mu^- \mu^- + \cancel{E}_T$ channel				
$e^-e^- \rightarrow W^-W^-$	$5.0 \times 10^{-3} \text{ fb}$	0.90	0.73	0.633
$e^-e^- \rightarrow W^-W^- \nu_e \nu_e$	$2.57 \times 10^{-2} \text{ fb}$	0.87	0.16	0.044

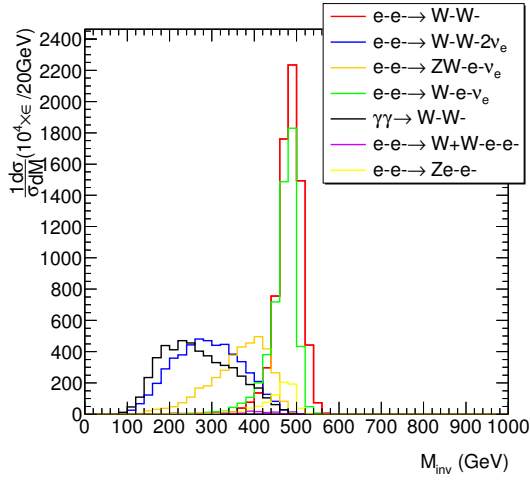
TABLE II: Cross-section and cut efficiencies in pure leptonic mode with $\sqrt{s} = 500 \text{ GeV}$

Process	σ	$\epsilon_{\text{tagging}}$	$\epsilon_{0.9 \text{ TeV} < m_{\text{inv}} < 1.9 \text{ TeV}}$	$\epsilon_{m_{\text{inv}} > 900 \text{ GeV}}$	$\epsilon_{m_{\text{inv}} > 700 \text{ GeV}}$	$\epsilon_{\cos \theta_{ll} < -0.95}$
$e^-e^- + \cancel{E}_T$ channel						
$e^-e^- \rightarrow W^-W^-$	0.18 fb	0.82	0.52	—	—	0.52
$e^-e^- \rightarrow W^-W^-\nu_e\nu_e$	1.3 fb	0.83	0.03	—	—	0.0018
$e^-e^- \rightarrow ZW^-e^-\nu_e$	1.15 fb	0.83	0.1	—	—	0.0024
$e^-e^- \rightarrow W^-e^-\nu_e$	124.5 fb	0.83	0.18	—	—	0.0173
$e^-e^- \rightarrow Ze^-e^-$	8 fb	0.82	0.29	—	—	0.152
$e^-\mu^- + \cancel{E}_T$ channel						
$e^-e^- \rightarrow W^-W^-$	0.37 fb	0.86	—	0.72	—	0.72
$e^-e^- \rightarrow W^-W^-\nu_e\nu_e$	2.6 fb	0.83	—	0.03	—	0.0018
$e^-e^- \rightarrow ZW^-e^-\nu_e$	1.15 fb	0.82	—	0.11	—	0.0027
$e^-e^- \rightarrow W^-e^-\nu_e$	124.5 fb	0.83	—	0.23	—	0.0222
$\mu^-\mu^- + \cancel{E}_T$ channel						
$e^-e^- \rightarrow W^-W^-$	0.18 fb	0.90	—	—	0.83	0.8208
$e^-e^- \rightarrow W^-W^-\nu_e\nu_e$	1.3 fb	0.82	—	—	0.06	0.0037

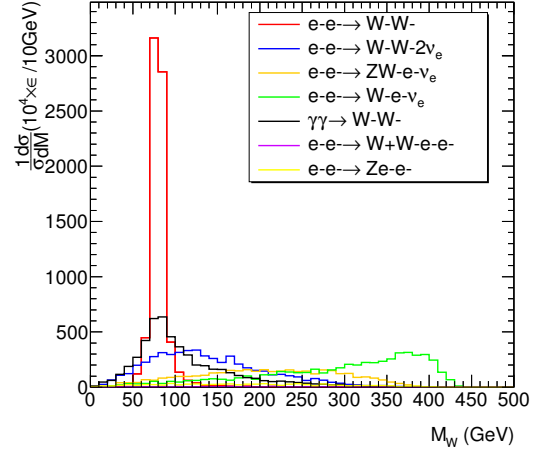
TABLE III: Cross-section and cut efficiencies in pure leptonic mode with $\sqrt{s} = 3 \text{ TeV}$

B. Semi-leptonic channel

The semi-leptonic channel are reconstructed with \cancel{E}_T . The system reconstructed with \cancel{E}_T and lepton is identified as a W boson, whose mass distribution could be used to cut out $W^-e^-\nu_e$ background in the $e^- + 2j + \cancel{E}_T$ channel. The $\gamma\gamma \rightarrow W^+W^-$ also contains reconstructable WW , but we are to use an invariant-mass cut to suppress it. In Fig.4a and Fig.4b, the two distributions in the $e^- + 2j + \cancel{E}_T$ channel are shown as a comparison. The $\gamma\gamma \rightarrow W^+W^-$ and $W^-e^-\nu_e$ processes can mimic the signal events respectively under m_W or m_{inv} cut, but not both. In the 3 TeV case, hadronic W is identified with j_W as have been discussed in the last section.



(a) m_{inv} distribution, $\sqrt{s} = 500$ GeV



(b) m_W distribution, $\sqrt{s} = 500$ GeV

FIG. 4: m_{inv} and m_W distributions of the reconstructed system in $e^- + 2j + \cancel{E}_T$ channel with $\sqrt{s} = 500$ GeV. ϵ is the tagging efficiencies

The two kinematic cuts are powerful in signal event selection and we list the efficiencies in Table.IV and V.

Process	σ	$\epsilon_{\text{tagging}}$	$\epsilon_{400 \text{ GeV} < m_{\text{inv}} < 550 \text{ GeV}}$	$\epsilon_{m_{\text{inv}} > 400 \text{ GeV}}$	$\epsilon_{70 < m_W < 90 \text{ GeV}}$
$e^- + 2j + \cancel{E}_T$ channel					
$e^-e^- \rightarrow W^-W^-$	$5.64 \times 10^{-2} \text{ fb}$	0.74	0.72	—	0.6
$e^-e^- \rightarrow W^-W^-\nu_e\nu_e$	0.23 fb	0.52	0.046	—	0.003
$e^-e^- \rightarrow ZW^-e^-\nu_e$	0.3 fb	0.37	0.13	—	0.002
$e^-e^- \rightarrow W^-e^-\nu_e$	537.3 fb	0.54	0.51	—	0.007
$e^-e^- \rightarrow W^+W^-e^-e^-$	0.23 fb	0.01	0.004	—	0.0002
$e^-e^- \rightarrow Ze^-e^-$	49.1 fb	0.08	0.07	—	0.003
$\gamma\gamma \rightarrow W^+W^-$	8 fb	0.51	0.037	—	0.006
$\mu^- + 2j + \cancel{E}_T$ channel					
$e^-e^- \rightarrow W^-W^-$	$5.64 \times 10^{-2} \text{ fb}$	0.74	—	0.72	0.6
$e^-e^- \rightarrow W^-W^-\nu_e\nu_e$	0.23 fb	0.52	—	0.05	0.002
$e^-e^- \rightarrow ZW^-e^-\nu_e$	0.1 fb	0.04	—	0.01	0.0004
$e^-e^- \rightarrow W^+W^-e^-e^-$	0.23 fb	0.037	—	0.0008	0.0001
$\gamma\gamma \rightarrow W^+W^-$	8 fb	0.49	—	0.04	0.003

TABLE IV: Cross-section and cut efficiencies in semi-leptonic channel with $\sqrt{s} = 500 \text{ GeV}$

Process	σ	$\epsilon_{\text{tagging}}$	$\epsilon_{m_{\text{inv}} > 2.5 \text{ TeV}}$
$e^- + j_W + \cancel{E}_T$ channel			
$e^-e^- \rightarrow W^-W^-$	2.2 fb	0.78	0.77
$e^-e^- \rightarrow W^-W^-\nu_e\nu_e$	13.2 fb	0.062	0.0032
$e^-e^- \rightarrow ZW^-e^-\nu_e$	9.1 fb	0.065	0.0064
$e^-e^- \rightarrow W^-e^-\nu_e$	774.5 fb	0.098	0.018
$e^-e^- \rightarrow W^+W^-e^-e^-$	1.143 fb	0.0013	0.0003
$e^-e^- \rightarrow Ze^-e^-$	15.76 fb	0.008	< 0.0001
$\gamma\gamma \rightarrow W^+W^-$	113 fb	0.006	0.0003
$\mu^- + j_W + \cancel{E}_T$ channel			
$e^-e^- \rightarrow W^-W^-$	2.2 fb	0.75	0.75
$e^-e^- \rightarrow W^-W^-\nu_e\nu_e$	13.2 fb	0.06	0.0026
$e^-e^- \rightarrow ZW^-e^-\nu_e$	2.4 fb	0.0034	< 0.0001
$e^-e^- \rightarrow W^+W^-e^-e^-$	1.143 fb	0.0009	0.0001
$\gamma\gamma \rightarrow W^+W^-$	113 fb	0.005	0.0002

TABLE V: Cross-section and cut efficiencies in semi-leptonic channel with $\sqrt{s} = 3 \text{ TeV}$

C. Hadronic channel

In the hadronic decay mode, the four jets are chosen to reconstruct two W bosons and the complete system. The invariant-mass distributions of each processes are shown in Fig.5. Though the two jet pairs with invariant mass around m_W could possibly be selected out, m_{4j} distributions of them deviate significantly from \sqrt{s} either because there're missed lepton or neutrino background final states or because the process is a photon-photon scattering.

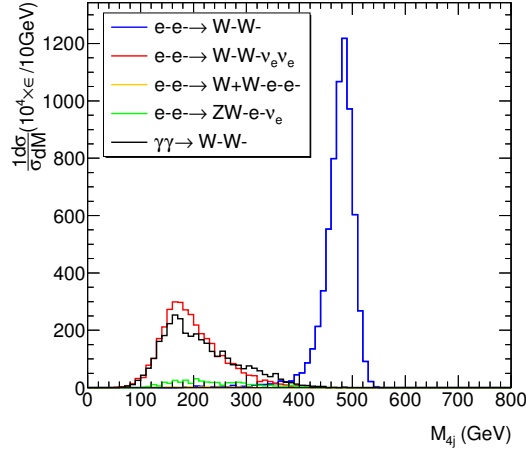


FIG. 5: m_{4j} distribution of the four-jet system, $\sqrt{s} = 500$ GeV. ϵ is the tagging efficiencies

In the $\sqrt{s} = 3$ TeV case, the tagging process requires two highly boosted W -jets with jet mass around m_W and cone size small enough. We further require the separation between two W -jets be larger than 0.4. The gauge bosons in e^-e^- background processes are not that boosted since electrons and neutrinos carry large energy. This is also true for $\gamma\gamma$ process because radiated photons are not that energetic as the electrons. We find the cone size values, which could be estimated with the separations between W hadronic decay final states, are in general larger in background events. Thus the background events can hardly meet the j_W tagging criteria. The detailed efficiencies are listed in the tables below.

Process	σ	$\epsilon_{\text{tagging}}$	$\epsilon_{m_{4j} > 400 \text{ GeV}}$
4j channel			
$e^-e^- \rightarrow W^-W^-$	0.16 fb	0.66	0.64
$e^-e^- \rightarrow W^-W^-\nu_e\nu_e$	0.5 fb	0.35	0.0006
$e^-e^- \rightarrow W^+W^-e^-e^-$	1 fb	0.004	0.0005
$e^-e^- \rightarrow ZW^-e^-\nu_e$	0.4 fb	0.04	0.0008
$\gamma\gamma \rightarrow W^+W^-$	34.4 fb	0.33	0.0031

TABLE VI: Cross-section and cut efficiencies in hadronic channel with $\sqrt{s} = 500$ GeV

Process	σ	$\epsilon_{\text{tagging}}$	$\epsilon_{m_{4j} > 2.3 \text{ TeV}}$
$2j_W$ channel			
$e^-e^- \rightarrow W^-W^-$	6.7 fb	0.73	0.73
$e^-e^- \rightarrow W^-W^-\nu_e\nu_e$	34.4 fb	0.011	0.0001
$e^-e^- \rightarrow W^+W^-e^-e^-$	6.3 fb	0.0001	< 0.0001
$e^-e^- \rightarrow ZW^-e^-\nu_e$	14.3 fb	0.0006	< 0.0001
$\gamma\gamma \rightarrow W^+W^-$	602 fb	0.0033	< 0.0001

TABLE VII: Cross-section and cut efficiencies in hadronic channel with $\sqrt{s} = 3 \text{ TeV}$

D. Detection possibility

We use the signal-to-background rate $\frac{S}{B}$ to evaluate the detection possibility of each channels. Those could potentially be detected are listed below

Process	$\frac{S}{B}, \sqrt{s} = 500 \text{ GeV}$	$\frac{S}{B}, \sqrt{s} = 3 \text{ TeV}$
$e^-\mu^- + \cancel{E}_T$	—	0.096
$\mu^-\mu^- + \cancel{E}_T$	2.80	30.72
$e^- + 2j/j_W + \cancel{E}_T$	—	0.12
$\mu^- + 2j/j_W + \cancel{E}_T$	1.38	28.81
$4j/2j_W$	0.95	74.44

TABLE VIII: Signal-to-Background rate. Hadronic W is identified as j_W in the 3 TeV case.

It's apparent that for the channels with more signal events survived than backgrounds, the detection is purely through event counting. In order to get the 5σ excess significance in the rest channels, the 3 TeV pure leptonic decay with $e^-\mu^-$, 3 TeV semi-leptonic decay with e^- and 500 GeV hadronic decay require about 1000 fb^{-1} , 130 fb^{-1} and 330 fb^{-1} data samples respectively.

In Fig.6, we show the comparison of $|V_{e2}|^2$ exclusion limit in the pure hadronic decay mode with the EWPO bound. We assume the luminosity could reach $\mathcal{L} = 500 \text{ fb}^{-1}$. In the 500 GeV case, the constraint is quite close to the present bound. The 3 TeV exclusion limit is significantly

lower, providing a chance to probe Majorana neutrinos beyond EWPO experiments.

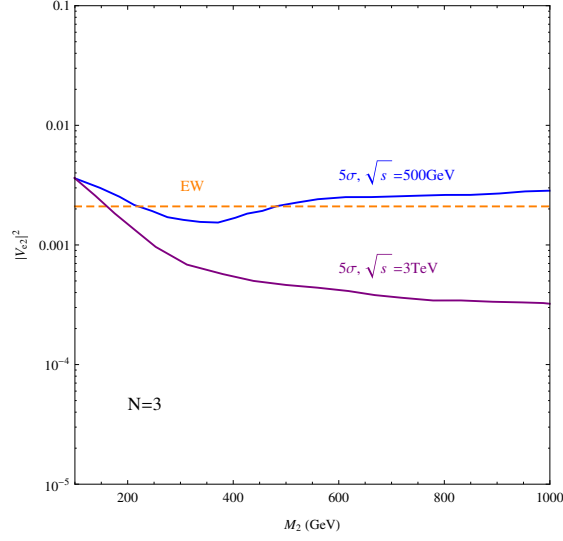


FIG. 6: 5σ exclusion limit of $|V_{e2}|^2$ and M_2 in hadronic mode

IV. CONCLUSION

In this study, we investigate how inverse $0\nu\beta\beta$ process on electron-electron colliders could be used to probe heavy Majorana neutrino. We demonstrate this idea with collider phenomenology analysis in all expected channels of W^-W^- decay and corresponding Monte Carlo simulation in the three Majorana neutrino flavor case. Among all the channels, the hadronic decay, semi-leptonic decay with μ^- and pure leptonic decay with $\mu^-\mu^-$ have the most detection potential, especially after the energy upgrade. The hadronic decay channel is expected to put constraint on $|V_{e2}|^2$ in future experiments.

V. ACKNOWLEDGEMENT

The work is supported in part by the National Science Foundation of China (11135006, 11275168, 11422544, 11075139, 11375151, 11535002) and the Zhejiang University Fundamental Research Funds for the Central Universities. KW is also supported by Zhejiang University

- [1] S. M. Bilenky and S. T. Petcov, Rev. Mod. Phys. **59** (1987) 671 Erratum: [Rev. Mod. Phys. **61** (1989) 169] Erratum: [Rev. Mod. Phys. **60** (1988) 575]. doi:10.1103/RevModPhys.59.671
- [2] S. M. Bilenky, C. Giunti, J. A. Grifols and E. Masso, Phys. Rept. **379**, 69 (2003) doi:10.1016/S0370-1573(03)00102-9 [hep-ph/0211462].
- [3] M. C. Gonzalez-Garcia and Y. Nir, Rev. Mod. Phys. **75**, 345 (2003) doi:10.1103/RevModPhys.75.345 [hep-ph/0202058].
- [4] H. F. Dylla and J. G. King, Phys. Rev. A **7**, 1224 (1973). doi:10.1103/PhysRevA.7.1224
- [5] J. Baumann, J. Kalus, R. Gahler and W. Mampe, Phys. Rev. D **37**, 3107 (1988). doi:10.1103/PhysRevD.37.3107
- [6] G. Barbiellini and G. Cocconi, Nature **329**, 21 (1987). doi:10.1038/329021b0
- [7] C. Q. Geng and R. E. Marshak, Phys. Rev. D **39**, 693 (1989). doi:10.1103/PhysRevD.39.693
- [8] K. S. Babu and R. N. Mohapatra, Phys. Rev. D **41**, 271 (1990). doi:10.1103/PhysRevD.41.271
- [9] S. Weinberg, Phys. Rev. Lett. **43**, 1566 (1979). doi:10.1103/PhysRevLett.43.1566
- [10] P. Minkowski, Phys. Lett. B **67**, 421 (1977). doi:10.1016/0370-2693(77)90435-X
- [11] R. N. Mohapatra and G. Senjanovic, Phys. Rev. Lett. **44**, 912 (1980). doi:10.1103/PhysRevLett.44.912
- [12] T. Yanagida, Conf. Proc. C **7902131**, 95 (1979).
- [13] M. Gell-Mann, P. Ramond and R. Slansky, Conf. Proc. C **790927**, 315 (1979) [arXiv:1306.4669 [hep-th]].
- [14] M. Agostini *et al.* [GERDA Collaboration], Phys. Rev. Lett. **111**, no. 12, 122503 (2013) doi:10.1103/PhysRevLett.111.122503 [arXiv:1307.4720 [nucl-ex]].
- [15] A. Gando *et al.* [KamLAND-Zen Collaboration], Phys. Rev. Lett. **110**, no. 6, 062502 (2013) doi:10.1103/PhysRevLett.110.062502 [arXiv:1211.3863 [hep-ex]].
- [16] L. Wolfenstein, Phys. Lett. B **107**, 77 (1981). doi:10.1016/0370-2693(81)91151-5
- [17] C. N. Leung and S. T. Petcov, Phys. Lett. B **145**, 416 (1984). doi:10.1016/0370-2693(84)90071-6
- [18] F. P. An *et al.* [Daya Bay Collaboration], Phys. Rev. Lett. **116**, no. 6, 061801 (2016) doi:10.1103/PhysRevLett.116.061801 [arXiv:1508.04233 [hep-ex]].
- [19] R. Aaij *et al.* [LHCb Collaboration], Phys. Rev. Lett. **112**, no. 13, 131802 (2014) doi:10.1103/PhysRevLett.112.131802 [arXiv:1401.5361 [hep-ex]].

- [20] D. Liventsev *et al.* [Belle Collaboration], Phys. Rev. D **87**, no. 7, 071102 (2013) doi:10.1103/PhysRevD.87.071102 [arXiv:1301.1105 [hep-ex]].
- [21] F. Bergsma *et al.* [CHARM Collaboration], Phys. Lett. B **166**, 473 (1986). doi:10.1016/0370-2693(86)91601-1
- [22] P. Vilain *et al.* [CHARM II Collaboration], Phys. Lett. B **343**, 453 (1995) [Phys. Lett. B **351**, 387 (1995)]. doi:10.1016/0370-2693(94)00440-I, 10.1016/0370-2693(94)01422-9
- [23] A. Vaitaitis *et al.* [NuTeV and E815 Collaborations], Phys. Rev. Lett. **83**, 4943 (1999) doi:10.1103/PhysRevLett.83.4943 [hep-ex/9908011].
- [24] G. Bernardi *et al.*, Phys. Lett. B **203**, 332 (1988). doi:10.1016/0370-2693(88)90563-1
- [25] A. V. Artamonov *et al.* [E949 Collaboration], Phys. Rev. D **91**, no. 5, 052001 (2015) Erratum: [Phys. Rev. D **91**, no. 5, 059903 (2015)] doi:10.1103/PhysRevD.91.059903, 10.1103/PhysRevD.91.052001 [arXiv:1411.3963 [hep-ex]].
- [26] J. Badier *et al.* [NA3 Collaboration], Z. Phys. C **31**, 341 (1986). doi:10.1007/BF01588030
- [27] S. A. Baranov *et al.*, Phys. Lett. B **302**, 336 (1993). doi:10.1016/0370-2693(93)90405-7
- [28] A. M. Cooper-Sarkar *et al.* [WA66 Collaboration], Phys. Lett. B **160**, 207 (1985). doi:10.1016/0370-2693(85)91493-5
- [29] E. Gallas *et al.* [FMMF Collaboration], Phys. Rev. D **52**, 6 (1995). doi:10.1103/PhysRevD.52.6
- [30] P. Astier *et al.* [NOMAD Collaboration], Phys. Lett. B **506**, 27 (2001) doi:10.1016/S0370-2693(01)00362-8 [hep-ex/0101041].
- [31] M. Aoki *et al.* [PIENU Collaboration], Phys. Rev. D **84**, 052002 (2011) doi:10.1103/PhysRevD.84.052002 [arXiv:1106.4055 [hep-ex]].
- [32] R. S. Hayano *et al.*, Phys. Rev. Lett. **49**, 1305 (1982). doi:10.1103/PhysRevLett.49.1305
- [33] P. Abreu *et al.* [DELPHI Collaboration], Z. Phys. C **74**, 57 (1997) [Z. Phys. C **75**, 580 (1997)]. doi:10.1007/s002880050370
- [34] G. Aad *et al.* [ATLAS Collaboration], JHEP **1507**, 162 (2015) doi:10.1007/JHEP07(2015)162 [arXiv:1506.06020 [hep-ex]].
- [35] V. Khachatryan *et al.* [CMS Collaboration], JHEP **1604**, 169 (2016) doi:10.1007/JHEP04(2016)169 [arXiv:1603.02248 [hep-ex]].
- [36] V. Khachatryan *et al.* [CMS Collaboration], Phys. Lett. B **748**, 144 (2015) doi:10.1016/j.physletb.2015.06.070 [arXiv:1501.05566 [hep-ex]].
- [37] F. F. Deppisch, P. S. Bhupal Dev and A. Pilaftsis, New J. Phys. **17**, no. 7, 075019 (2015)

- doi:10.1088/1367-2630/17/7/075019 [arXiv:1502.06541 [hep-ph]].
- [38] M. Drewes and B. Garbrecht, arXiv:1502.00477 [hep-ph].
 - [39] A. Atre, T. Han, S. Pascoli and B. Zhang, JHEP **0905**, 030 (2009) doi:10.1088/1126-6708/2009/05/030 [arXiv:0901.3589 [hep-ph]].
 - [40] S. Antusch and O. Fischer, JHEP **1410**, 094 (2014) doi:10.1007/JHEP10(2014)094 [arXiv:1407.6607 [hep-ph]].
 - [41] B. Ananthanarayan and P. Minkowski, Phys. Lett. B **373**, 130 (1996) doi:10.1016/0370-2693(96)00128-1 [hep-ph/9512271].
 - [42] T. G. Rizzo, Phys. Lett. B **116**, 23 (1982). doi:10.1016/0370-2693(82)90027-2
 - [43] D. London, G. Belanger and J. N. Ng, Phys. Lett. B **188**, 155 (1987). doi:10.1016/0370-2693(87)90723-4
 - [44] D. A. Dicus, D. D. Karatas and P. Roy, Phys. Rev. D **44**, 2033 (1991). doi:10.1103/PhysRevD.44.2033
 - [45] G. Belanger, F. Boudjema, D. London and H. Nadeau, Phys. Rev. D **53**, 6292 (1996) doi:10.1103/PhysRevD.53.6292 [hep-ph/9508317].
 - [46] J. Gluza and M. Zralek, Phys. Rev. D **52**, 6238 (1995) doi:10.1103/PhysRevD.52.6238 [hep-ph/9502284].
 - [47] J. Gluza and M. Zralek, Phys. Lett. B **362**, 148 (1995) doi:10.1016/0370-2693(95)01158-M [hep-ph/9507269].
 - [48] J. Gluza and M. Zralek, Phys. Lett. B **372**, 259 (1996) doi:10.1016/0370-2693(96)00074-3 [hep-ph/9510407].
 - [49] C. Greub and P. Minkowski, eConf C **960625**, NEW149 (1996) [Int. J. Mod. Phys. A **13**, 2363 (1998)] doi:10.1142/S0217751X98001153 [hep-ph/9612340].
 - [50] W. Rodejohann, Phys. Rev. D **81**, 114001 (2010) doi:10.1103/PhysRevD.81.114001 [arXiv:1005.2854 [hep-ph]].
 - [51] S. Banerjee, P. S. B. Dev, A. Ibarra, T. Mandal and M. Mitra, Phys. Rev. D **92**, 075002 (2015) doi:10.1103/PhysRevD.92.075002 [arXiv:1503.05491 [hep-ph]].
 - [52] T. Asaka and T. Tsuyuki, Phys. Rev. D **92**, no. 9, 094012 (2015) doi:10.1103/PhysRevD.92.094012 [arXiv:1508.04937 [hep-ph]].
 - [53] C. G. Lester and D. J. Summers, Phys. Lett. B **463** (1999) 99 [hep-ph/9906349].
 - [54] V. M. Budnev, I. F. Ginzburg, G. V. Meledin and V. G. Serbo, Phys. Rept. **15**, 181 (1975). doi:10.1016/0370-1573(75)90009-5

- [55] J. Alwall, M. Herquet, F. Maltoni, O. Mattelaer and T. Stelzer, JHEP **1106**, 128 (2011) doi:10.1007/JHEP06(2011)128 [arXiv:1106.0522 [hep-ph]].
- [56] T. Sjostrand, S. Mrenna and P. Z. Skands, JHEP **0605**, 026 (2006) doi:10.1088/1126-6708/2006/05/026 [hep-ph/0603175].